THE JOURNAL OF BIOLOGICAL CHEMISTRY Vol. 275, No. 41, Issue of October 13, pp. 32016–32026, 2000
Printed in U.S.A.

Functional and Structural Characterization of Synthetic HIV-1 Vpr That Transduces Cells, Localizes to the Nucleus, and Induces G_2 Cell Cycle Arrest*

Received for publication, May 11, 2000, and in revised form, July 3, 2000
Published, JBC Papers in Press, July 19, 2000, DOI 10.1074/jbc.M004044200

Peter Henklein‡§, Karsten Bruns§¶‖, Michael P. Sherman§, Uwe Tessmer¶, Kai Licha‡‡, Jeffrey Kopp§§, Carlos M. C. de Noronha§, Warner C. Greene**, Victor Wray¶, and Ulrich Schubert¶ ¶¶‖‖**

*From the ‡Humboldt University, Institute of Biochemistry, 10115 Berlin, the ¶University of Hamburg, Heinrich-Pette-Institute of Experimental Virology and Immunology, 20251 Hamburg, ‖Gesellschaft für Biotechnologische Forschung, Department of Molecular Structure Research, 38124 Braunschweig, Germany, the **Gladstone Institute of Virology and Immunology, University of California, San Francisco, California, the ‡‡Institute of Diagnostic Research GmbH, Free University, Berlin, Germany, the §§NIDDKD, Kidney Disease Section, Laboratory of Viral Diseases, and ¶¶NIAID, Laboratory of Viral Diseases, National Institutes of Health, Bethesda, Maryland 20892*

Human immunodeficiency virus (HIV) Vpr contributes to nuclear import of the viral pre-integration complex and induces G_2 cell cycle arrest. We describe the production of synthetic Vpr that permitted the first studies on the structure and folding of the full-length protein. Vpr is unstructured at neutral pH, whereas under acidic conditions or upon addition of trifluorethanol it adopts α-helical structures. Vpr forms dimers in aqueous trifluorethanol, whereas oligomers exist in pure water. ^{1}H NMR spectroscopy allows the signal assignment of N- and C-terminal amino acid residues; however, the central section of the molecule is obscured by self-association. These findings suggest that the *in vivo* folding of Vpr may require structure-stabilizing interacting factors such as previously described interacting cellular and viral proteins or nucleic acids. In biological studies we found that Vpr is efficiently taken up from the extracellular medium by cells in a process that occurs independent of other HIV-1 proteins and appears to be independent of cellular receptors. Following cellular uptake, Vpr is efficiently imported into the nucleus of transduced cells. Extracellular addition of Vpr induces G_2 cell cycle arrest in dividing cells. Together, these findings raise the possibility that circulating forms of Vpr observed in HIV-infected patients may exert biological effects on a broad range of host target cells.

Human immunodeficiency virus type 1 (HIV-1)[1] is a lentivirus that encodes the canonical retroviral Gag, Pol, and Env proteins, as well as six regulatory or auxiliary proteins including Tat, Rev, Vpu, Vif, Nef, and Vpr. Although not essential for viral replication in tissue culture, the latter four proteins are highly conserved and likely exert important but less well understood functions *in vivo* that contribute to viral pathogenesis. Vpr, a ~14-kDa, 96-amino acid protein, is conserved among the primate lentiviruses HIV-1, HIV-2, and the simian immunodeficiency virus, supporting the notion that it plays an important role in the viral life cycle *in vivo*. Indeed, deletion of *vpr* and the related *vpx* genes in simian immunodeficiency virus severely compromises the pathogenic properties in experimentally infected rhesus macaques (1, 2).

Vpr has important biological properties that may facilitate viral replication, including the presence of at least two nuclear localization signals (3–7). Unlike most animal retroviruses, the primate lentiviruses are able to replicate efficiently in nondividing cells. Although not essential for viral replication in T cells, *in vitro* Vpr significantly augments viral replication in terminally differentiated monocytes/macrophages, a function that probably relates to its karyophilic property (3). Vpr is thought to participate in the import of the viral pre-integration complex, facilitating its passage across the nuclear pore. This import may similarly involve the function of other karyophilic viral proteins including the $p17^{gag}$ matrix and integrase proteins (reviewed in Refs. 8 and 9).

Vpr also induces G_2 cell cycle arrest in infected proliferating human T cells (reviewed in Refs. 8, 10, and 11). Such G_2 arrest may serve to induce an intracellular milieu that is more favorable for long terminal repeat-directed transcription (12). In fact, sufficient quantities of Vpr are present within the viral particle to induce G_2 arrest prior to the *de novo* synthesis of provirally derived proteins (13, 14). Other biological activities ascribed to Vpr include ion channel formation (15), transcriptional activation of various heterologous promoters (16–19), co-activation of the glucocorticoid receptor (20), regulation of cell differentiation (10), and induction of apoptosis (21, 22). The importance of these latter functions for maintenance of the HIV replicative life cycle and the induction of disease in the infected host remains uncertain.

The participation of Vpr in HIV-1 replication suggests that selective interruption of Vpr function with small molecule inhibitors might yield a new class of antiviral agents. However,

* This work was supported by National Institutes of Health Grant R01 AI45324 (to W. C. G.), and Schu11/2-1 and a Heisenberg grant from the Deutsche Forschungsgemeinschaft (to U. S.). The costs of publication of this article were defrayed in part by the payment of page charges. This article must therefore be hereby marked "*advertisement*" in accordance with 18 U.S.C. Section 1734 solely to indicate this fact.

§ These authors contributed equally to this work.
‖‖ To whom correspondence should be addressed: Laboratory of Viral Diseases, Rm. 205, Bldg. 4, 4 Center Dr., MSC 0440, NIH, Bethesda, MD 20892-0440. Tel.: 301-496-7880; Fax: 301-402-7362; E-mail: uschubert@nih.gov.

[1] The abbreviations used are: HIV-1, human immunodeficiency virus, type 1; TFE, trifluorethanol; DMEM, Dulbecco's modified Eagle's medium; DTT, dithiothreitol; PBS, phosphate-buffered saline; HPLC, high pressure liquid chromatography; Fmoc, *N*-(9-fluorenyl)methoxycarbonyl; DMF, dimethyl formamide; ESI, electrospray ionization; MS, mass spectrometry; DLS, dynamic light scattering; PAGE, polyacrylamide gel electrophoresis; *s*Vpr, synthetic Vpr; SPPS, solid phase peptide synthesis; MALDI/TOF, matrix-assisted laser desorption ionization/time-of-flight.

the design of effective Vpr antagonists requires more detailed knowledge of its molecular structure, function, and mode of action. The availability of essentially unlimited quantities of pure and biologically active Vpr could certainly accelerate progress in understanding its biological functions and propel the development of effective antagonists. Recombinant Vpr has been produced in insect cells and as a glutathione *S*-transferase fusion protein in *Escherichia coli* (15). At concentrations as low as 100 pg/ml, the extracellular addition of recombinant Vpr activates HIV-1 replication in both leukemic cell lines and primary peripheral blood mononuclear cells (23, 24). However, when maintained at high concentrations as required for structural investigation, preparations of recombinant Vpr often undergo spontaneous aggregation. In addition, a cytotoxic effect of the protein in both pro- and eukaryotic cells (25, 26) limits production of Vpr by recombinant genetics.

We now describe the production of synthetic Vpr (*s*Vpr), its purification to homogeneity, and the characterization of this synthetic protein by N-terminal sequencing, mass spectrometry (MS), and gel electrophoresis. In addition, we report the behavior of *s*Vpr in aqueous solution under various conditions as analyzed by dynamic light scattering (DLS), CD, and ^{1}H NMR spectroscopy. Finally, we demonstrate that *s*Vpr is efficiently taken up by human macrophages and HeLa cells from the extracellular medium, is imported into the nucleus of such transduced cells, and induces G_2 cell cycle arrest.

EXPERIMENTAL PROCEDURES

Peptide Synthesis and Purification—*S*ynthesis was performed on a PerkinElmer Life Sciences MilliGen 9050 automated peptide synthesizer on a 0.09-mmol scale on a TentaGel R PHB Ser(*t*-butyl) Fmoc resin (capacity 0.19-mmol g^{-1}) using the Fmoc/*t*-butyl strategy. The following side chain protecting groups were used: 2,2,4,6,7-pentamethyldihydrobenzofurane-5-sulfonyl (Arg), *t*-butoxycarbonyl (Trp and Lys), *t*-butyl ether (Thr, Ser, and Tyr), *t*-butyl ester (Asp and Glu), and trityl (Asn, Cys, Gln, and His). Couplings were performed with *N*-[1*H*-benzotriazol(1-yl)(dimethylamino)methylene]-*N*-methylmethanaminium hexafluorophosphate-*N*-oxide (HBTU), except that 1-(1-pyrrolidinyl-1*H*-1,2,3-triazolo-[4,5-*b*-]-pyridin-1-ylmethylene)-pyrrolidinium hexafluorophosphate-*N*-oxide was used for the last 30 amino acids in order to increase the efficiency of the final part of the synthesis (27). Coupling was performed with 1 mmol Fmoc amino acids using HBTU in *N*-methylpyrrolidone as coupling agent with a cycle time of 45 min for single coupling and 75 min for double coupling applied for the last 56 amino acids. In order to avoid aspartimide formation, deprotection of the N-terminal Fmoc group was performed with piperidine/DMF/formic acid during the entire course of the synthesis. Deprotection of the Fmoc group was performed during the complete synthesis with 20% piperidine in DMF, containing 0.1 M HCOOH to avoid aspartimide side reactions. The crude protein was purified by reverse phase HPLC on a Vydac C18 column (40 × 300 mm, 1520 μm, 300 Å) with a linear gradient of 100% solvent A to 100% solvent B in 53 min (solvent A, 1000 ml of water, 2 ml of trifluoroacetic acid; solvent B, 500 ml of acetonitrile, 100 ml water, 1 ml of trifluoroacetic acid) at a flow rate of 100 ml min^{-1} with spectrophotometric monitoring at λ = 214 nm. The fractions were analyzed by reverse phase HPLC (Shimadzu L10) on a Vydac C18 column (4.6 × 250 mm, 5 μm, 300 Å) with a linear gradient of 10–100% solvent B over 45 min. The peptide $Vpr^{47–96}$ was synthesized under the same conditions, and the synthesis of peptide $Vpu^{32–81}$ has been described (28).

Fluorescent Labeling of sVpr—*s*Vpr was labeled with Alexa 488 labeling kit (A-10235, Molecular Probes). The manufacturer's procedure was modified as follows: 2 mg of *s*Vpr was dissolved in 1 ml of DMF; 1 vial of dye from the kit was added; and the pH was adjusted to 8.5–9.0 with diisopropylethylamine. After a 2-h incubation at room temperature, the reaction was diluted with water, and the pH was adjusted to 2.0. Labeled *s*Vpr was purified on the resin supplied with the kit. For flow cytometry, *s*Vpr was labeled with the fluorescent dye bis-1,1′-(4-sulfobutyl)indodicarbocyanine-5-carboxylic acid (sodium salt) that was coupled in the last step of the peptide synthesis to the N-terminal NH_2 of *s*Vpr by incubating the resin with the peptide in DMF with HBTU and diisopropylethylamine overnight. After completion, the resin was washed with DMF and methylene chloride, dried, and treated with 90% trifluoroacetic acid, 5% triisopropylsilane, and 5% water. Trifluoroacetic acid was then removed under vacuum, and *s*Vpr was precipitated with diethyl ether purified by a standard HPLC procedure. This procedure selectively labels the N-terminal residue, leaving other side chains of the peptide functional, and allows a relatively easy purification of the peptide while still attached to the resin. Similar to Cy3, this novel fluorescent dye absorbs at 550 nm and emits at 585 nm. Its detailed synthesis will be described elsewhere.

Peptide Sequencing and Mass Spectrometry—For *s*Vpr, 30 sequencing steps were completed on an Applied Biosystems 473A pulsed liquid phase sequencer according to a standard protocol. Positive ion ESI mass spectra were recorded on a triple quad Finnigan TSQ 700 mass spectrometer equipped with an electrospray source. Protein samples were dissolved in 70% aqueous methanol and infused at a flow rate of 1 μl min^{-1} into the electrospray chamber with an ES needle voltage of 5.5 kV. The experimental spectrum showing multiply charged molecular ions with 8–13 positive charges was deconvoluted with standard software. MALDI/TOF mass spectra were recorded on a Bruker reflex MALDI/TOF mass spectrometer using an N_2 laser (337 nm).

Light-scattering Measurements—DLS was performed on a DynaPro-801 Molecular Sizing Instrument. Protein solutions (250 μl) prepared either in water or in 50% aqueous TFE at a concentration of ~3.5 mg ml^{-1} (*s*Vpr) or 4 mg ml^{-1} ($Vpr^{47–96}$) were injected through 0.1-μm Whatman membrane filters. Samples were illuminated by a semiconductor laser (780 nm, 25 milliwatts) generated by a miniature solid state $Ga_{1-y}Al_yAs$ diode. The photons scattered at a 90° angle by the particles in the sample were collected by an avalanche photodiode, and the time-dependent fluctuation in intensity of the scattered light was analyzed. The translational diffusion coefficient D_T was calculated with the manufacturer's software (Dynamics, version 2.1). D_T was then used to calculate the degree of sample polydispersity and the hydrodynamic radius of gyration R_H of the particles using the Stokes-Einstein equation: $(R_H = (k_bT)\cdot(6\pi\eta D_T)^{-1}$, where k_b is Boltzman's constant; T is absolute temperature in Kelvin, and η = solvent viscosity. M_r was calculated on a standard curve (M_r *versus* R_H) supplied by the manufacturer. Ten continuous measurements were made for each sample.

CD Spectroscopy—CD spectra were recorded at room temperature in 0.5-mm cuvettes on a Jasco J-600 spectropolarimeter in a wavelength range from 260 to 180 nm, and the resulting curves were smoothed with a high frequency filter. Samples of sVpr and $Vpr^{47–96}$ were dissolved at a concentration of 0.2 mg ml^{-1} under various solution conditions (TFE concentration, pH). Secondary structure content was quantified with the program VARSELEC.

^{1}H NMR Spectroscopy—Samples of the protein were dissolved in distilled water containing 10% D_2O or containing 50% aqueous TFE-D_2 by volume to give a final volume of 0.6 ml. Spectra were recorded at 300 K on a Bruker Avance DMX 600 NMR spectrometer. The ^{1}H spectra were referenced to sodium 4,4-dimethyl-4-silapentane-1-sulfonate or internally to the residual methylene signal of TFE at 3.95 ppm. Two-dimensional phase-sensitive spectra of ^{1}H COSY (correlation spectroscopy), TOCSY (total correlation spectroscopy), with mixing times of 110 ms, and NOESY (nuclear Overhauser and exchange spectroscopy), with mixing times of 250 ms, were recorded without spinning and processed with standard Bruker software.

Antibodies, SDS-PAGE, Western Blot, and Immunoprecipitation—A rabbit polyclonal antiserum, *R-96*, was generated by immunization with *s*Vpr. Immunoprecipitation of *s*Vpr was carried out in Triton wash buffer (50 mM Tris/HCl, pH 7.4, 60 mM NaCl, 0.5% Triton X-100), pre-cleared with non-immune human and rabbit sera, followed by incubation with *R-96* antibodies pre-loaded onto GammaBind-Plus-Sepharose beads. The immunoprecipitates were washed twice with Triton wash buffer, once with SDS-DOC buffer (50 mM Tris/HCl, pH 7.4, 300 mM NaCl, 0.1% SDS, 0.1% deoxycholate), boiled for 10 min at 95 °C in sample buffer (2% SDS, 1% mercaptoethanol, 1% glycerol, 65 mM Tris/HCl, pH 6.8), and subjected to electrophoresis on 16% Prosieve SDS-PAGE gels. Virus stocks were generated in HeLa cells transfected with pNL4-3 (29) and subsequently used to infect MT 4 cells. Virions were pelleted from cell culture supernatant (30,000 × *g*, 1.5 h, 4 °C) and purified on a sucrose cushion. For immunoblotting, samples were transferred to Immobilon polyvinylidene difluoride membranes (Immobilon). Membranes were incubated with *R-96,* and binding of the antibodies was identified with ^{125}I-labeled protein G.

Cellular Uptake of sVpr—sVpr and $Vpu^{32–81}$ were iodinated by the chloramine-T method. Briefly, ~20 μg of peptides were reacted with 5.5×10^7 Bq (1.5 mCi) $Na^{125}I$. Free iodine was removed by gel filtration through a Dowex ion exchange column saturated with bovine serum albumin. For studies on cellular uptake, rat yolk choriocarcinoma L2-

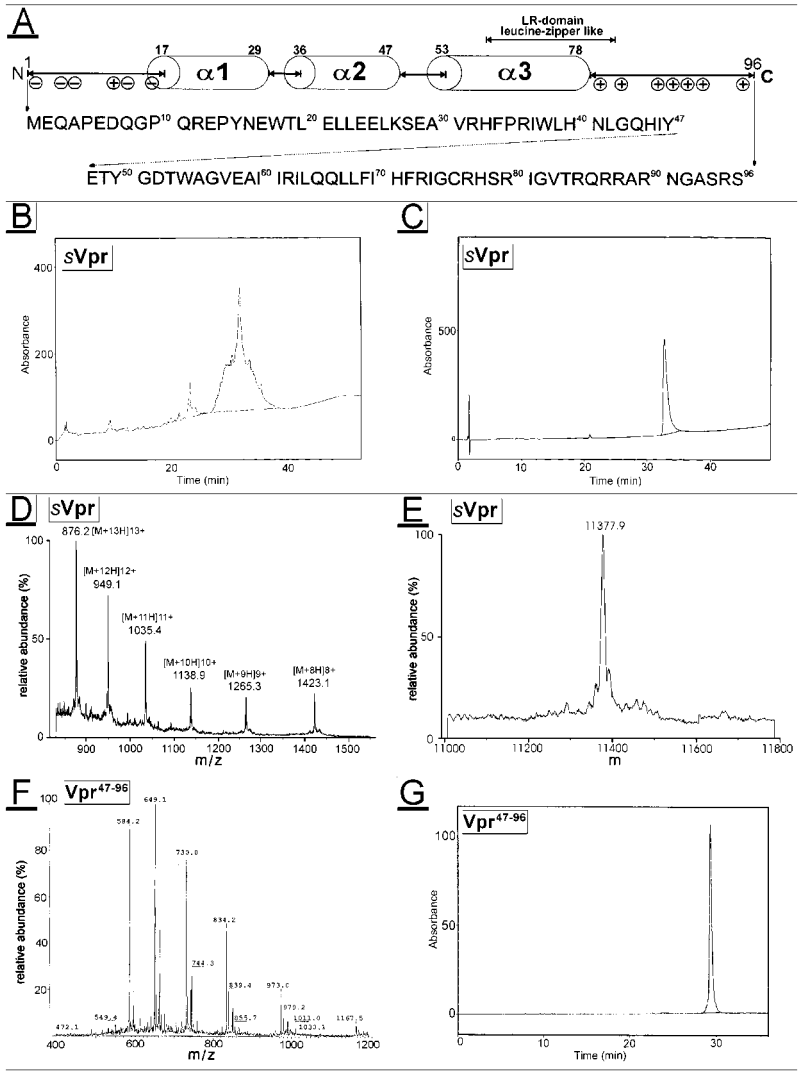

FIG. 1. **Synthesis, purification, and MS analysis of *s*Vpr and the C-terminal fragment Vpr$^{47–96}$.** *A,* primary sequence of *s*Vpr derived from the isolate HIV-$1_{NL4–3}$ is shown *below* the model of secondary structures identified in Vpr fragments (36, 39). Positively or negatively charged residues at the termini, helical structures, and a leucine-rich (*LR*) zipper-like motif that is presumably involved in the oligomerization of Vpr are indicated. Chromatograms of crude (*B*) or purified (*C*) *s*Vpr obtained by reverse-phase acetonitrile gradient HPLC are shown, with UV detection at 214 nm. *D,* positive ion ESI mass spectra of purified *s*Vpr, experimental mass spectrum showing the distribution of multiply charged ions. *E,* deconvoluted mass spectrum showing the intense envelope of the molecular ion at 11,377.9 Da. *F,* experimental ESI mass spectra; *G,* chromatogram of purified Vpr$^{47–96}$.

RYC cells were grown in Dulbecco's modified Eagle's medium (DMEM) with 10% (v/v) fetal bovine serum to 75% confluence on 24-well plates. Cells were washed once with phosphate-buffered saline (PBS) and incubated in serum-free DMEM supplemented with 0.1% bovine serum albumin and ^{125}I-labeled *s*Vpr or, as a negative control, ^{125}I-labeled Vpu$^{32–81}$. Radioactive peptides were added to the medium at a specific activity of 18 kBq ml^{-1}. In parallel, cells were also treated with a 100-fold excess of unlabeled *s*Vpr or Vpu$^{32–81}$. Cells were incubated for specified times at 37 °C, and the distribution of intra- and extracellular radioactivity was determined as described (30). Briefly, medium was removed, and the cell layer was washed with PBS and lysed with 1% Triton X-100 in PBS. Radioactivity was determined in triplicate in the medium and cell layer. To correct for nonspecific binding of peptides to the cell surface, the cell layer radioactivity determined at time point 0 min (time when radiolabeled peptides were added to the medium for less than 30 s) was subtracted as background from the radioactivity detected in the cell layer.

For cellular localization studies, either a suspension of HeLa cells (2×10^6 ml^{-1}) or a confluent monolayer of human macrophages cultivated in chamber slides was incubated with fluorescent *s*Vpr-488. After 48 h, the cells were washed with PBS, fixed with 1% paraformaldehyde for 10 min, and mounted. The specimens were examined by epifluorescence or scanning confocal microscopy (model MRC-600; Bio-Rad). Macrophages were isolated from random HIV-1-seronegative healthy blood donors. First, peripheral blood mononuclear cells were isolated using Ficoll-Paque (Amersham Pharmacia Biotech) and grown in slide chambers, containing DMEM, 10% fetal calf serum, and 10% human serum AB (Gemini Bio-Products). After 1 week, cells were washed, and the adherent monolayer of monocyte-derived macrophages was used for import studies with *s*Vpr. The number of cells transduced by *s*Vpr-Cy3 was estimated by flow cytometry.

Cell Cycle Analysis—HeLa cells were incubated with *s*Vpr-Cy3 for 48 h, trypsinized, and fixed for 30 min in 2% formaldehyde followed by incubation with 1 mg ml^{-1} RNase A and 10 μg ml^{-1} propidium iodide in PBS for 30 min. Cellular DNA content in the fixed cells was then assessed with a FACScan flow cytometer and analyzed with the ModFit LT program (Becton Dickinson).

RESULTS

Synthesis and Purification of sVpr—Solid phase peptide synthesis (SPPS) of full-length Vpr was performed with a sequence derived from the isolate HIV-$1_{NL4–3}$ (Fig. 1*A*). HPLC profiles of the crude and purified protein products are shown in Fig. 1, *B* and *C*, respectively. In contrast to a recently described SPPS procedure for the synthesis of a Vpr protein derived from a different HIV-1 isolate (31), we optimized the procedure with respect to the use of coupling agents, protection groups, cleavage reagents, and duration of coupling reactions. Our protocol gave reproducibly high yields (usually 15%) of purified *s*Vpr without encountering any of the previously reported (31) synthesis problems such as incomplete coupling and deprotection, inter- and intrachain reaction with the resin matrix, hydrogen bond-mediated peptide aggregation, or side chain reactions. We also synthesized various fragments of *s*Vpr using the same SPPS protocol. The HPLC purification of the peptide Vpr$^{47–96}$, comprising the C-terminal domain of *s*Vpr from positions Tyr-47 to Ser-96, is demonstrated in Fig. 1*G*.

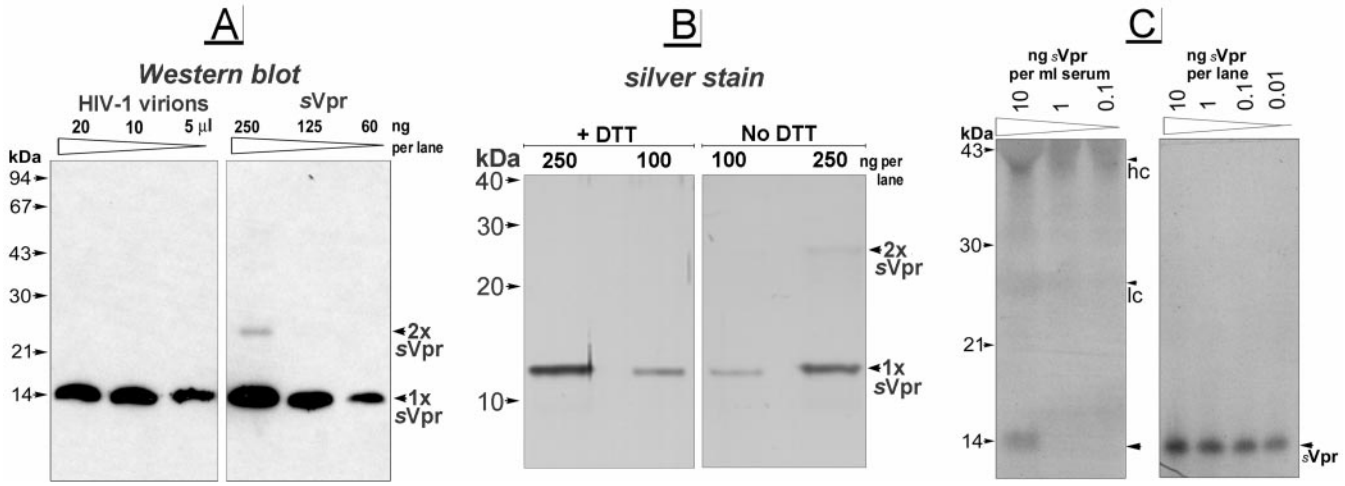

FIG. 2. **Characterization of *s*Vpr by SDS-PAGE, Western blot, and immunoprecipitation.** *A,* a serial dilution of 250–60 ng of *s*Vpr or 20–5 μl of lysates of HIV-1 virions per lane were separated by SDS-PAGE on 16% gels, transferred to polyvinylidene difluoride membrane, and stained with *R-96* antibodies. Antibody binding was visualized by ECL reaction. Positions of molecular weight standard marker proteins are indicated to the *left*, and positions of monomers and dimers of *s*Vpr are indicated to the *right. B,* silver-stained 18% SDS-PAGE after separation of 250 and 100 ng of *s*Vpr in the presence or absence of 250 mM DTT. *C, s*Vpr (0.1–10 ng) was mixed with human serum and immunoprecipitated with *R-96* antibodies. Immunoprecipitates were separated by SDS-PAGE on 14% gels, electrotransferred, and analyzed by Western blot with *R-96* antibodies and ^{125}I-protein G for detection. On the *right panel*, *s*Vpr (0.01–10 ng per lane) was directly separated in the gel before Western blot analysis. Autoradiograms of a 2-day exposure are shown in both panels.

Analysis of sVpr by Protein Sequencing, MS, and Western Blotting—The identity of purified *s*Vpr was confirmed by sequencing of the N-terminal 30 amino acids. Positive ion ESI MS was used for molecular weight determination. The experimental data showed a well defined multiply charged spectrum (Fig. 1*D*) that was deconvoluted to give an intense envelope for the molecular ion cluster at a molecular mass of 11,377.9 Da (Fig. 1*E*), corresponding exactly with the molecular mass of 11,377.9 Da calculated for *s*Vpr. In addition, the correct molecular mass of *s*Vpr was also established by MALDI/TOF mass spectrometry that showed an intense molecular ion cluster at 11,377.2 Da (not shown). In summary, the MS and sequence analyses indicated that *s*Vpr was homogenous and showed no detectable evidence of by-products. Similar results were also obtained for the C-terminal fragment Vpr$^{47–96}$. The peptide was purified to homogeneity (Fig. 1*G*), and the correct molecular mass of 5829.7 Da was established by ESI MS (Fig. 1*F*).

Molecular properties of *s*Vpr were further characterized by SDS-PAGE (Fig. 2). Dilutions of *s*Vpr were separated and detected by Western blotting using Vpr-specific antibodies. For comparison with viral Vpr, lysates of purified HIV-1 particles were analyzed in parallel (Fig. 2*A*). In agreement with sequencing and MS data, *s*Vpr migrated as a single band with an apparent molecular mass of ~14 kDa that was almost indistinguishable from the migration of viral Vpr. Western blot (Fig. 2*A*) or direct silver staining of *s*Vpr in SDS-PAGE (Fig. 2*B*) did not detect peptide fragments that could have resulted from proteolysis or incomplete synthesis.

In addition to monomeric Vpr, a small percentage of *s*Vpr was detected in an M_r range consistent with dimers and trimers. Such candidate oligomers were only detected at concentrations of ≥250 ng of *s*Vpr per lane (Fig. 2*A*). The fact that *s*Vpr forms oligomers (as shown below by DLS) is consistent with the previous demonstration of Vpr oligomers by chemical cross-linking (32). These multiple forms were not observed with preparations of viral Vpr (Fig. 2*A*). Two possibilities may explain these results. First, according to the detection of monomeric *s*Vpr by Western blot, the highest amount of viral Vpr analyzed corresponded to ~125 ng of *s*Vpr per lane; at this concentration multimers of *s*Vpr were not detected. Second, physical interactions between the C-terminal p6^{gag} domain of the Pr55 Gag polyprotein (33, 34) direct the incorporation of Vpr into budding virus particles (35). Hence, the presence of at least one of the known Vpr binding partners, p6^{gag}, in the virus preparation may prevent homo-oligomerization of viral Vpr that was otherwise evident for isolated *s*Vpr.

Vpr contains a single cysteine at residue 76 that may potentially participate in intermolecular disulfide bond formation. Although disulfide-bridged dimers have not been reported for viral or recombinant Vpr, SDS-PAGE analysis of *s*Vpr in the absence of reducing agents indicated that ~10% of the molecules exist as disulfide-linked dimers, the formation of which was prevented by the addition of dithiothreitol (DTT) (Fig. 2*B*).

*s*Vpr was also used as an immunogen in rabbits to generate polyclonal anti-Vpr antibodies. The titer of the anti-Vpr antibody, *R-96*, was significantly increased when standard coupling of *s*Vpr to keyhole limpet hemocyanin was omitted indicating that the peptide presents a *bona fide* antigen. The resultant *R96* antiserum reacts with Vpr proteins from several different HIV-1 isolates and binds to both virus-derived Vpr and *s*Vpr with comparable efficiency. Furthermore, using *R96* for immunoprecipitation *s*Vpr was detected at concentrations as low as 10 ng ml^{-1} diluted in human serum (Fig. 2*C*). Together, these findings demonstrate the usefulness of *R96* for detection of viral Vpr in serum samples of HIV-infected individuals (23).

DLS Analysis of Vpr—Our SDS-PAGE results (Fig. 2, *A* and *B*) and the previously published cross-linking data (32) suggest that Vpr tends to form oligomeric structures. To study the oligomerization of *s*Vpr in its dynamic state in solution, as opposed to the artificial fixation of particular folding states by chemical cross-linking, we used DLS to examine *s*Vpr under various solution conditions. In pure water at a concentration of ~3.5 mg ml^{-1} and without pH adjustment (pH ~3.0), deconvolution of the primary DLS data indicates the existence of at least two components with R_H values of ~4.8 and 26.2 nm (with relative abundance of 99 and 1%) corresponding to complexes with molecular masses of 128 and 8075 kDa, respectively. Thus, in aqueous solution, *s*Vpr existed as high order aggregates (~decamers) with a lower percentage of higher multimers. Such oligomers of *s*Vpr cannot be resolved by SDS-PAGE and may not be stabilized by cross-linking as demonstrated

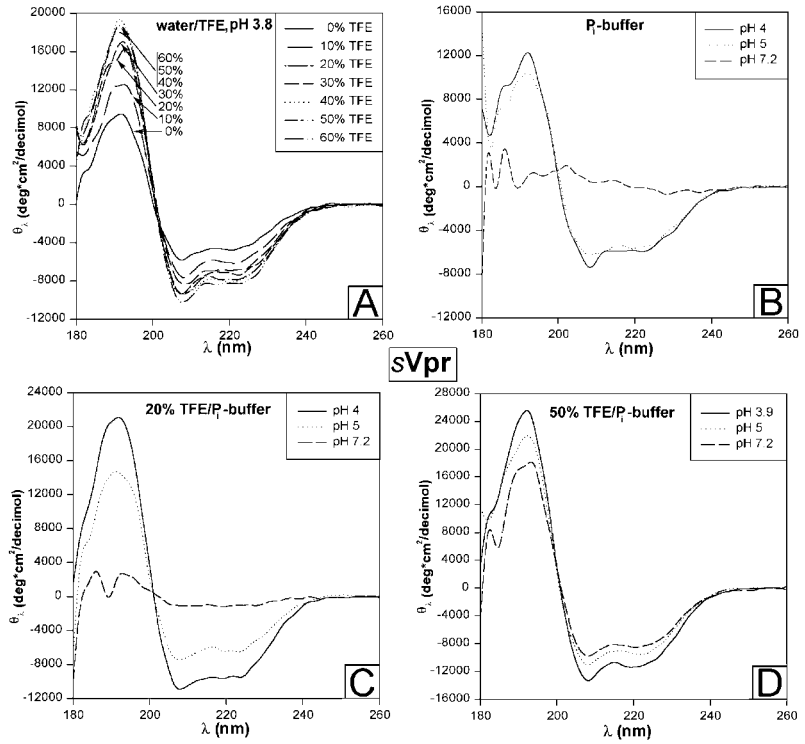

FIG. 3. **Far-ultraviolet CD spectra of *s*Vpr.** Spectra were recorded in pure water at different TFE concentrations (*A*), at different pH values in P_i buffer alone (*B*), or with 20% (*C*) or 50% TFE (*D*).

before (32). Although the majority of *s*Vpr exists in high M_r aggregates, we observed no precipitation of the peptide, even at the relatively high mM concentration range investigated.

Next we tested whether oligomers of *s*Vpr could be reduced by an organic solvent such as TFE, which favors intramolecular interactions and suppresses hydrophobic intermolecular interactions that were implied to drive Vpr clustering (36). DLS data acquired in 50% TFE showed that *s*Vpr exists as a single species with a particle size that deviates less than 15% from the average R_H of 2.3 nm. This value corresponds well to a molecular mass of 26 kDa and indicates that TFE induces the formation of stable *s*Vpr dimers. Thus, the addition of TFE promotes a substantial loss of oligomers and the formation of dimers. This could result from changes in secondary structure that reduce the tendency for aggregation or from suppression of hydrophobic interactions by TFE.

Recently, it was suggested that a leucine-rich domain located within the C-terminal α-helix of Vpr provides the molecular constraints for homo-oligomerization of Vpr (36). We therefore investigated whether the C-terminal fragment, $Vpr^{47–96}$ (Fig. 1, *G* and *F*), also tends to self-associate. DLS analysis of $Vpr^{47–96}$ at a concentration of ~4 mg ml^{-1} in pure water showed a single component (98.5% abundance) with an R_H value of ~3 nm corresponding to a hexameric particle of ~43 kDa. Upon addition of 50% TFE, one major species (94.2% abundance) of monomer (R_H = 1.25 and 6.25 kDa) and small amounts of dimers and trimers were detected. These data indicate that, like full-length *s*Vpr, the C-terminal fragment $Vpr^{47–96}$ exhibits an inherent tendency for oligomerization that depends on the hydrophobicity of the solvent.

Characterization of sVpr by CD Spectroscopy—To analyze further the effect of TFE on secondary structures in *s*Vpr, we investigated the peptides by CD spectroscopy under various solution conditions. Initially, *s*Vpr was analyzed in water alone, without buffer, at a pH of ~3.8. The corresponding CD curve demonstrated negative ellipticity at 208 and 222 nm, and a strong positive band at ~192 nm (Fig. 3*A*). These findings suggested the presence of significant content of α-helical structure, accounting for ~18% according to deconvolution of the CD spectrum. Addition of up to 20% TFE resulted in an initial stabilization of these helical structures (up to ~31% helical content), whereas further addition of TFE up to 60% induced smaller changes with the maximum helical content at approximately 50% TFE. In contrast to previous studies of Vpr protein fragments (36–39), our findings suggest that the full-length peptide *s*Vpr possesses structure even in pure water and that its helical structure is stabilized but not induced by TFE.

Compared with the calculated basic isoelectric point, it was surprising that solutions of *s*Vpr adopt a helical configuration at acidic pH since this is inconsistent with the physiological pH present in the cytosol or nucleus of the cell where native Vpr is predominantly expressed. Hence, we analyzed *s*Vpr at a constant concentration in phosphate buffer (P_i) while varying the pH from 3.9 to 7.2 (Fig. 3*B*). Remarkably, while increasing pH up to 5.0 had almost no effect, at neutral pH 7.2 the protein adopted a completely random conformation. This transition occurred at a critical pH of approximately 5.0, although some loss in the shape of CD curves started at pH 6.0 (data not shown), and deprivation of structure was complete at neutral pH. In agreement with the DLS measurements, no precipitation of *s*Vpr was evident under any of the solution conditions investigated.

Subsequently, we tested whether the destabilizing effect of neutral pH on *s*Vpr structure could be reversed by addition of TFE, an agent that appears to have a subtle effect on the peptide structure at acidic pH. Addition of 20% TFE, which had near-maximal effect at pH 3.8 (Fig. 3*A*), did not stabilize *s*Vpr at neutral pH (Fig. 3*C*). However, TFE concentrations as high as 50% clearly provided an environment where the helical structure of *s*Vpr was present (Fig. 3*D*), even at the critical neutral pH where *s*Vpr exhibited no structure without TFE (Fig. 3*B*). In 50% TFE, the change from pH 4 to 7.2 had only a small effect upon the CD curves, implying that the secondary structure remained intact and was only slightly destabilized on transition to the higher pH (Fig. 3*D*).

Recent structural studies on a 51-residue N-terminal fragment of Vpr revealed no consequences of pH variation on secondary structure (39). These findings implied that the struc-

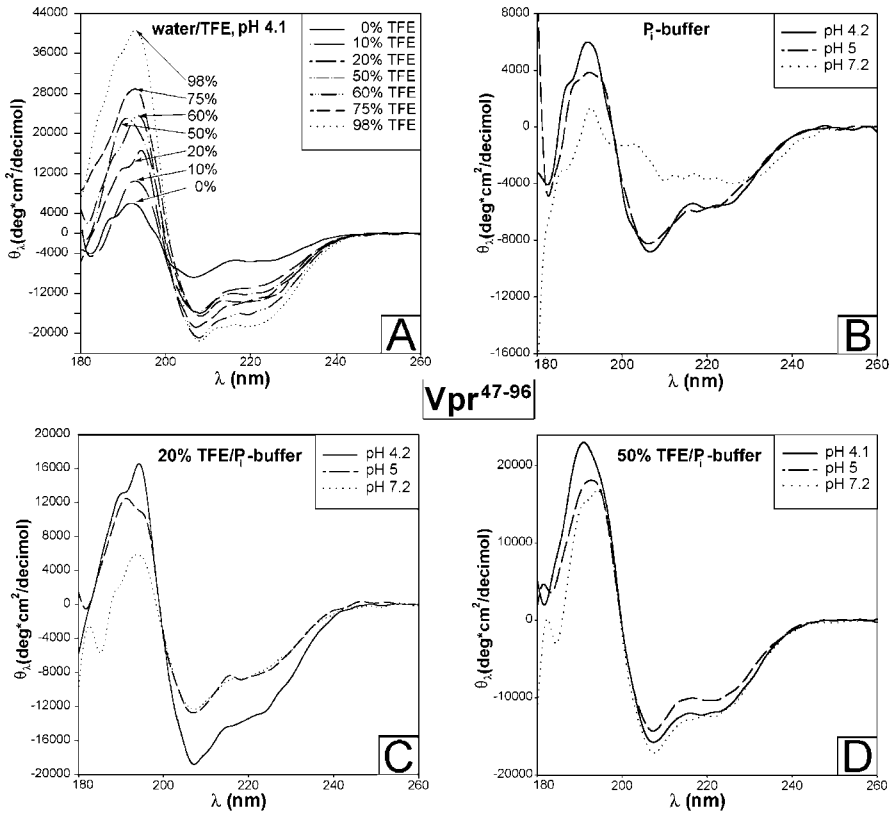

FIG. 4. **Far-ultraviolet CD spectra of Vpr$^{47–96}$ recorded in pure water at different TFE concentrations (*A*) and at different pH values in P$_i$ buffer alone (*B*) or with 20 (*C*) or 50% TFE (*D*).**

tural motif contributing to the pH-dependent folding of *s*Vpr (Fig. 3) may be located within the C-terminal domain of Vpr. To test this hypothesis, we subjected the fragment Vpr$^{47–96}$ (Fig. 1, *F* and *G*) to an identical CD analysis (Fig. 4). Like *s*Vpr, Vpr$^{47–96}$ adopted an acidic pH of 4.1 in pure water and tended to have a helical conformation, although not as pronounced as for *s*Vpr (Fig. 4*A*). Addition of TFE increased the helical content, but in contrast to *s*Vpr, there was a linear response with TFE concentration that reached a maximum at 98% TFE. As with *s*Vpr, a pH-dependent folding switch was observed for Vpr$^{47–96}$ at pH 5.0 (Fig. 4*B*). The effect of TFE was slightly different to the situation of *s*Vpr as the unfolding of Vpr$^{47–96}$ could be reversed to some extent by the addition of 20% TFE (Fig. 4*C*). Again, in 50% TFE solution, the destabilizing effect of neutral pH was almost absent (Fig. 4*D*). Thus, the folding of the C-terminal fragment responded to changes in solvent conditions in a fashion similar to that of full-length *s*Vpr.

In summary, solution conditions can profoundly affect the structure of full-length Vpr. The peptide is completely unstructured at neutral pH, whereas lowering the pH to a critical threshold of pH 5.0 or adding a membrane mimetic, such as TFE, stabilizes secondary structure that is mainly α-helical in character. This phenomenon can be attributed, at least partially, to structures located in the C terminus, most likely in the leucine-rich domain of Vpr.

^{1}H NMR Spectroscopic Characterization of sVpr—The structure of *s*Vpr was further analyzed by ^{1}H NMR spectroscopy under various solution conditions. One- and two-dimensional ^{1}H NMR spectra were recorded in water alone without any salt or buffer at pH 3.1 and in 50% aqueous TFE-D_2. Stable solutions of *s*Vpr devoid of any sign of protein precipitation were obtained at concentrations considerably higher than those employed in the CD measurements. The one-dimensional spectra of *s*Vpr (Fig. 5) showed relatively broad lines for both solutions, although the majority of those in water alone were the broadest. This is readily seen in the low field region of the spectrum where line widths of 10–12 Hz were measured for the Trp-N^{1}H signals at 9.4–9.9 ppm in the 50% TFE solution (Fig. 5*B*), but these lines were not visible in the spectrum obtained in pure water (Fig. 5*C*).

SDS-PAGE analysis (Fig. 2*B*) indicated that a small fraction of *s*Vpr forms disulfide-linked dimers. However, the addition of an equimolar amount of DTT gave no visible alteration in the NMR spectrum, suggesting that the majority of the molecules was not present as disulfide-linked dimers. However, it must be remembered that the NMR data were obtained using a protein solution at pH ~3, and the SDS-PAGE was performed at pH 6.8. Consequently the signal broadening (Fig. 5), indicative of protein-protein interaction, most likely arises from non-covalent associations for which a leucine-zipper motif in the C terminus has been implicated (36).

The one- and two-dimensional NMR spectra (Figs. 5 and 6) show a further phenomenon; in both pure aqueous as well as 50% TFE solutions the protein has some regions that show particularly broad lines, whereas at least several parts of the molecule appear to be relatively flexible resulting in sharper lines. Thus, inspection of two-dimensional TOCSY spectra at different contour levels (Fig. 6) indicates that there are several residues with resolvable spin systems. NOESY spectra of *s*Vpr in 50% TFE indicate that these signals belong to the first 7 N-terminal (Glu-2 to Gln-8) and 5 C-terminal (Gly-92 to Ser-96) residues of the protein (Fig. 6*A*). Similarly, in water alone and at a lower concentration of *s*Vpr, the C-terminal residues Gly-82 to Thr-84 and Gly-92 to Arg-95 were unambiguously identified (Fig. 6*B*).

Extracellular sVpr Transduces Cells and Localizes to the Nucleus—Next, we sought to investigate the biological activity of *s*Vpr. Like the HIV-1 Tat protein (40), extracellular Vpr appears to exhibit certain functions in HIV-1 host cells. Recombinant Vpr or Vpr isolated from the serum of patients displaying high HIV-1 loads enhances viral replication in both HIV-infected cell lines and primary human peripheral blood

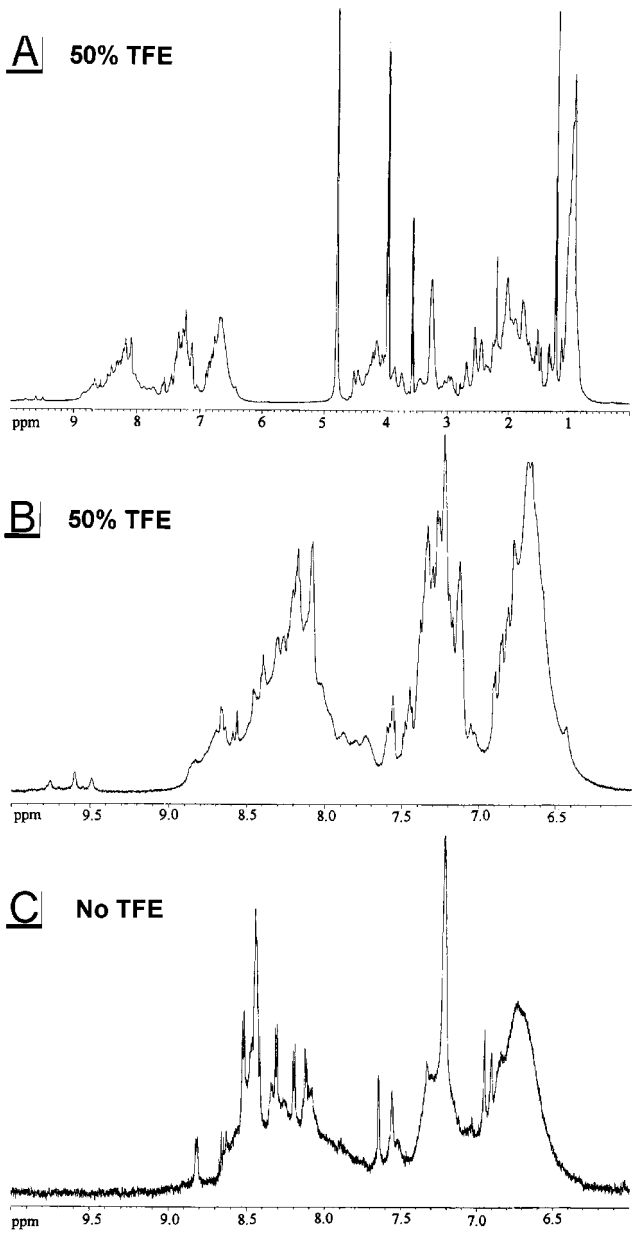

FIG. 5. **One-dimensional ^{1}H NMR spectrum of *s*Vpr.** *A,* ^{1}H NMR spectrum in 50% TFE. *B,* the low field region of the same spectrum. *C,* the corresponding low field region of the ^{1}H NMR spectrum of *s*Vpr in water alone.

mononuclear cells (23, 24). Furthermore, recombinant Vpr added to cell culture medium appears to exert glucocorticoid-like effects (22). However, it has not been formally determined whether virion-free Vpr actually enters cells or instead engages cell-surface receptors and initiates various signaling cascades. To address these questions and to test the biological activity of *s*Vpr, we studied cellular uptake and localization of *s*Vpr. The peptide was labeled with the fluorophor Alexa-488, and the resulting peptide, *s*Vpr-488, was used to monitor uptake and subcellular localization of the peptide in both macrophages and HeLa cells. These studies revealed that *s*Vpr-488 effectively entered cells following its addition in the extracellular medium (in a process termed as protein transduction) and further accumulated in the nucleus of these transduced cells (Fig. 7). This intracellular staining pattern was not observed with a 10-fold higher concentration of a labeled control peptide ($p6^{gag}$-488) or the un-conjugated fluorescent dye itself (data not shown). Confocal microscopy revealed that in HeLa cells the transduced peptide *s*Vpr-488 appears to be occasionally concentrated in cytosolic spots, whereas the majority of the peptide was clearly localized in the nucleus (Fig. 7, *C* and *D*). These data, together with our preliminary observation that *s*Vpr activates HIV-1 replication and is specifically incorporated into budding HIV-1 virions (data not shown), provide evidence that *s*Vpr possesses biological activities similar to those of viral Vpr.

Receptor-independent Uptake of sVpr—We next analyzed the specificity of *s*Vpr cellular uptake. Because Vpr is cationic at physiological pH, we considered the possibility that its uptake is mediated by megalin, a cell-surface receptor that is expressed in a variety of tissues that binds to positively charged molecules (41). In the carcinoma cell line L2-RYC, which expresses large amounts of megalin, we found significant and time-dependent uptake of *s*Vpr (Fig. 8). The level of intracellular *s*Vpr reached a maximum of 8–10% within 2 h followed by a constant plateau for up to 16 h. This plateau may reflect a steady state between uptake and secretion of radioactivity. In contrast, a 50-amino acid control peptide, Vpu^{32-81}, synthesized under the same conditions as full-length *s*Vpr and containing similar secondary structural elements (28) was not effectively internalized (Fig. 8). Similar results were also obtained in HeLa cells. Furthermore, the uptake of ^{125}I-labeled *s*Vpr was not inhibited by a 100-fold excess of unlabeled *s*Vpr (Fig. 8), suggesting that this process either does not involve a saturable receptor system or alternatively is mediated through a very high capacity receptor system.

sVpr Is Transduced Efficiently and Induces G_2 Cell Cycle Arrest—Transfection of various proliferating human cells with expression vectors encoding HIV-1 Vpr produces G_2 cell cycle arrest in a majority of the transfected cells (10). Given the nucleophilic properties of *s*Vpr, we investigated whether cells transduced with extracellularly added *s*Vpr undergo a similar cell cycle arrest. HeLa cells were incubated with *s*Vpr labeled with a Cy3-like fluorophor that allows effective sorting of the transduced cells. When *s*Vpr-Cy3 was added at concentrations of 2, 5, and 10 μg ml^{-1}, flow cytometric studies revealed dose-dependent uptake of *s*Vpr-Cy3 from the medium (71, 92, and 97% of the cells, respectively) (Fig. 9*A*). When cells were incubated with *s*Vpr-Cy3 at 2 μg ml^{-1} and sorted based on fluorescence, 30% of the positive cells were arrested in the G_2/M phase of the cell cycle. In contrast, only 13% of cells of the non-transduced cell population were present in G_2/M (Fig. 9*B*). These data strongly suggest that *s*Vpr is biologically active and is able to induce G_2 cell cycle arrest in susceptible cells.

DISCUSSION

Synthesis of Full-length Vpr—Biological and structural studies of Vpr have been hampered by the limited availability of purified protein due to the inherent propensity of Vpr to participate in homo- and heteromolecular interactions leading to aggregation. Although partial sequences of Vpr have been synthesized for biological (25, 26) and structural studies (36–38), chemical synthesis of full-length soluble forms of Vpr has proven difficult. For example, a Vpr peptide derived from the HIV-1_{BRU} sequence has been synthesized, but irreversible aggregation precluded purification of the product (42–44). The biological activity of such forms of Vpr could not be analyzed in solution. Far-Western blotting demonstrated the binding of SDS-denatured Vpr to the viral nucleocapsid $p7^{NC}$ (43), a finding not recapitulated with virus-derived Vpr (34). The optimized SPPS protocol we have now described permits the synthesis of soluble Vpr in sufficient quantities to allow structural and biological analyses. This approach also circumvents the

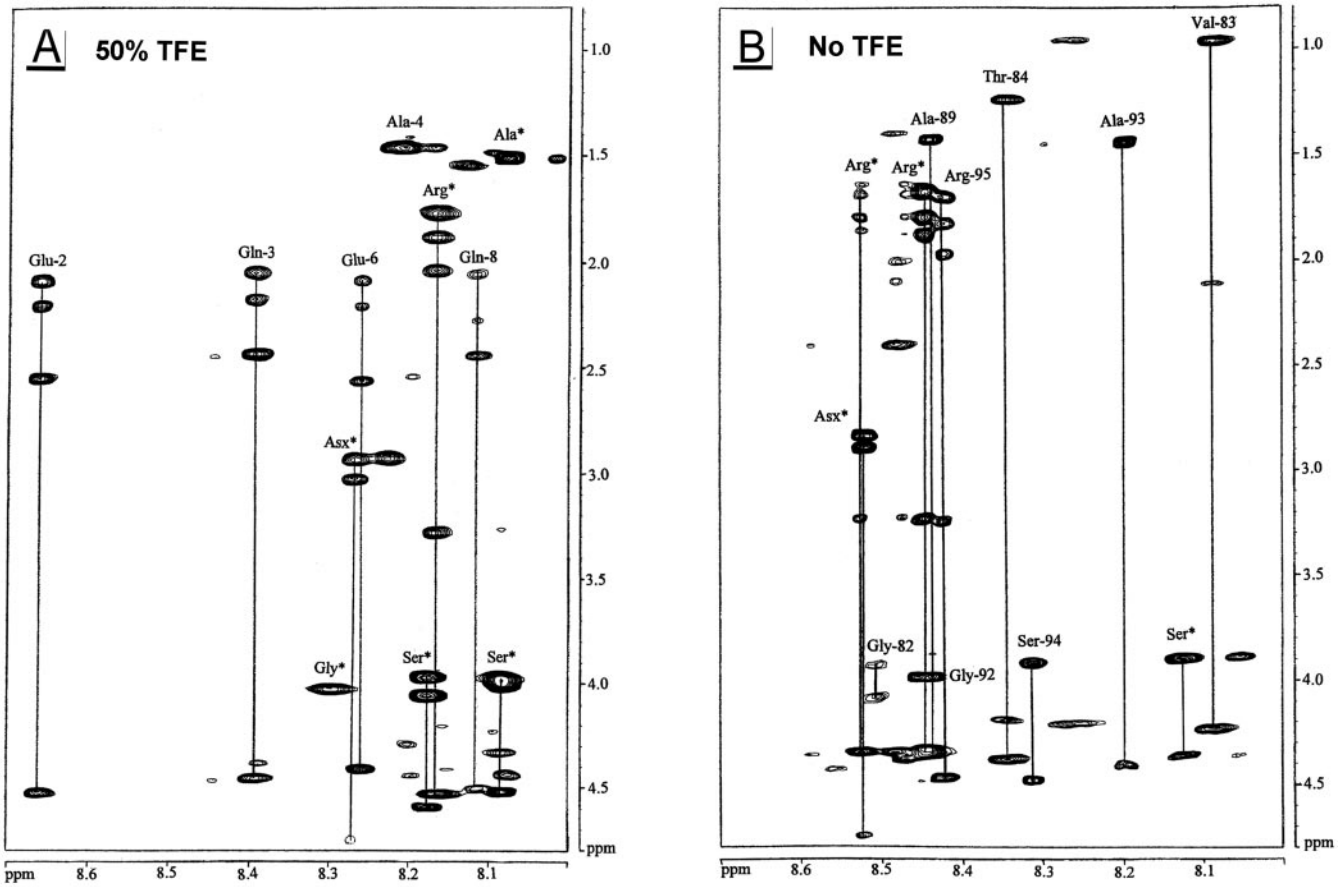

FIG. 6. **Two-dimensional ^{1}H TOCSY spectrum of *s*Vpr.** NH region of the two-dimensional TOCSY spectrum of *s*Vpr in 50% TFE (*A*) and in water alone (*B*) displayed to show the sharp signals. Signal assignments are those described in the text.

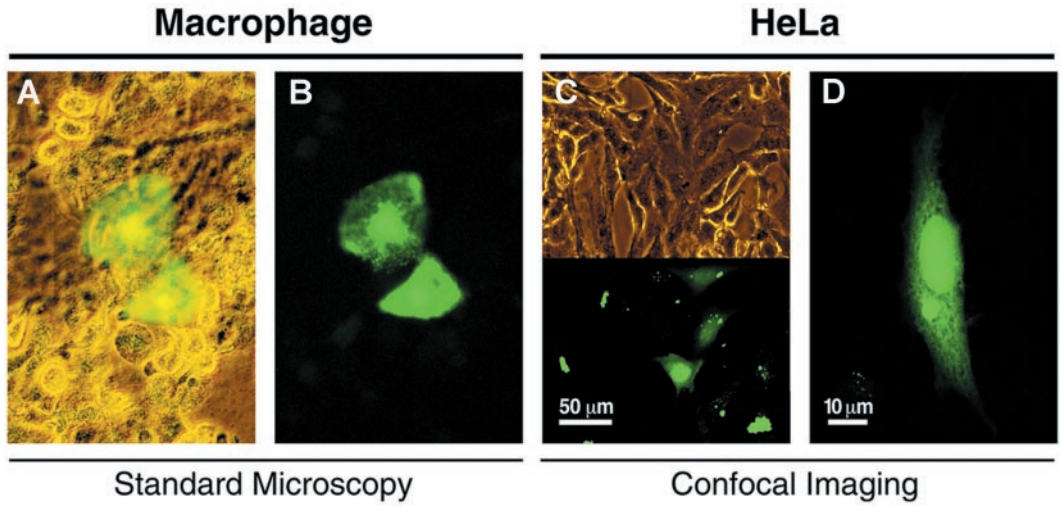

FIG. 7. **Cellular uptake and intracellular localization of *s*Vpr-488.** Fluorescently labeled peptide *s*Vpr-488 at a concentration of 0.1 μg/ml was added to human macrophages (*A* and *B*) or HeLa cells (*C* and *D*). After 48 h, cells were fixed and examined by phase contrast (*A*) and epifluorescence (*B*) microscopy or by scanning confocal microscopy using phase contrast (*C, top*) or epifluorescence (*C, bottom,* and *D*).

cytotoxic effects and attendant low yields obtained when Vpr is expressed in either prokaryotic or eukaryotic cells (21, 22, 25). Although other authors (31) have claimed that Vpr is difficult to synthesize due to its tendency for incomplete coupling, matrix interaction, and peptide aggregation, we did not encounter any of these difficulties by using optimized Fmoc chemistry with no additional side chain protection.

Effect of Solution Conditions on Structure and Oligomerization of sVpr—Several attempts have been made to identify and characterize the structural and functional domains of Vpr. This protein appears to contain at least four discrete structural domains as follows: a negatively charged N terminus, a central domain comprised of three helices (N-terminal α-1 and α-2 and C-terminal α-3), and a positively charged C terminus (Fig. 1*A*). The best characterized region, α-3 (residues 53–78), overlaps with a leucine-rich domain that contains a short leucine zipper-

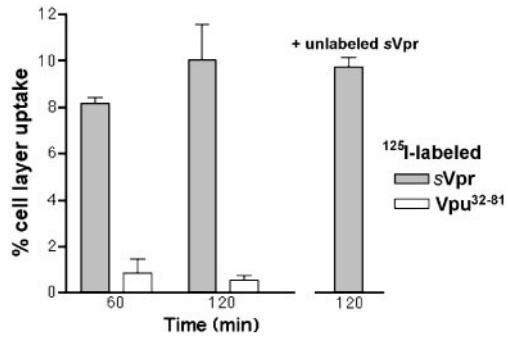

FIG. 8. **Receptor-independent uptake of *s*Vpr.** L2 cells were incubated with ^{125}I-labeled *s*Vpr or Vpu$^{32-81}$ (control) for 60 or 120 min, and the distribution of radioactivity in the cell layer and the medium was determined in triplicate. In parallel, cells were incubated for 120 min with ^{125}I-labeled *s*Vpr and a 100-fold molar excess of unlabeled *s*Vpr.

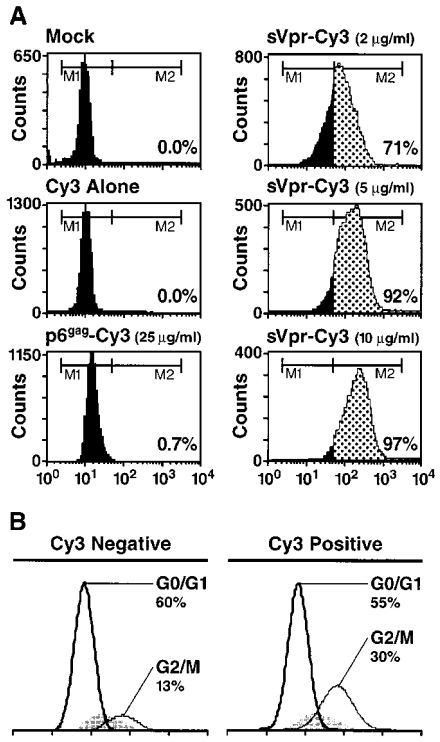

FIG. 9. **sVpr transduction and induction of G_2 cell cycle arrest.** *A,* HeLa cells were incubated in medium containing *s*Vpr-Cy3 or similarly labeled p6^{gag}-Cy3 at the indicated concentrations, fixed, stained with propidium iodide, and analyzed by flow cytometry. There was a dose-dependent uptake of sVpr-Cy3 whereas no p6^{gag}-Cy3 was found staining the cells. *B,* cell cycle analysis of HeLa cells incubated with 2 μg/ml *s*Vpr-Cy3 shows significantly more Cy3-positive cells than Cy3-negative cells in the G_2/M phase.

like motif involved in self-association (36, 45). The assignment of functional domains largely derives from mutational analyses and is complicated by variable results. Nuclear localization and cell cycle arrest have been assigned to different domains in Vpr, although mutations throughout the length of Vpr can alter various properties of this protein (4, 25, 38, 45, 46). Structural analyses of Vpr fragments have relied on CD and NMR spectroscopy. In all cases, the membrane mimetic organic solvent TFE or micelle solutions were employed to obtain suitable solution conditions that afford structure-stabilizing effects. Full-length *s*Vpr based on HIV-1$_{BRU}$ has been studied in 30% TFE, although structural details have not been reported (31).

Our initial NMR experiments on *s*Vpr in water alone and in 50% TFE identified line broadening for ^{1}H signals from the central section of the molecule, and two-dimensional data allowed sequential assignments of only a limited number of C- or N-terminal residues. To gain further insights into the folding characteristics of *s*Vpr, we conducted DLS and CD studies of *s*Vpr in various solutions. In pure water and in the absence of other binding partners, *s*Vpr formed large complexes that preserved a significant amount of α-helical structure at low pH. Above pH 5.0, the structure became random. Remarkably, this pH-induced switch was minimized by the addition of TFE. Thus, TFE has three pronounced effects on *s*Vpr as follows: it prevents large complex formation, stabilizes secondary structure at low pH, and protects this secondary structure against disruption at physiologic pH. These characteristics are consistent with the tendency of Vpr to interact with other molecules, including cellular and viral proteins (reviewed in Ref. 8) or even HIV-1-derived DNA (36, 47). These interactions may, like TFE or low pH, stabilize structure and folding of Vpr.

Cellular Uptake and Nuclear Translocation of sVpr—It was important to demonstrate that *s*Vpr exhibited biological activities similar to that characteristic of native Vpr. Indeed, *s*Vpr displayed nucleophilic properties similar to virus-derived Vpr or Vpr expressed in transfected cells. Furthermore, *s*Vpr also induced G_2 cell cycle arrest in human cells. Perhaps most surprisingly, *s*Vpr mediated these effects even when added to the extracellular medium of cell cultures. Biological functions have been attributed to extracellular Vpr, but it was unknown whether Vpr actually can enter cells independent of the viral context. Our findings are the first evidence that isolated molecules of Vpr alone can effectively transduce cells and exert a biological effect.

The HIV-1 Tat protein has also been shown to contain an effective protein transduction domain (40, 48). Recent *in vivo* studies have demonstrated that the 11-amino acid protein transduction domain from Tat can be fused to a variety of proteins thereby promoting their cellular uptake in an array of different cell types including neurons (49, 50). This finding suggests that Vpr and Tat might share similar protein transduction properties. It is likely that the unusual dipole character of Vpr, in combination with the C-terminal basic residues, regulates binding of Vpr to charges on membrane phospholipids and that cell uptake may be mediated by amphipathic helices present in Vpr. The protein transduction domain of Tat has recently been localized to the sequence YGKKRRQRRR, which strongly resembles the motif RQRRAR centered in the basic C terminus of Vpr (48). Interestingly, this arginine-rich domain is part of a slightly larger domain (residues 73–96) sufficient for nuclear translocation of a heterologous cytoplasmic protein through a novel low energy, RanGTP-independent pathway of nuclear import (4). It has been proposed that there are at least two import signals contained within Vpr, one consisting of the leucine-rich helices and one present in the basic C-terminal region (4). It will be interesting to identify the structural motifs that mediate transport through the cell membrane and determine how this mechanism relates to the function of nuclear import and export signals present in Vpr.

Extracellular Vpr can be detected in the serum and cerebrospinal fluid of HIV-1-infected patients, presumably at levels comparable to capsid p24^{gag} protein (23). Vpr is selectively incorporated into virus particles by interacting with the C-terminal p6^{gag} domain of the Pr55 Gag precursor (35). Considering the assumption that the majority of serum Vpr derives from disintegration of virus particles (23), it is conceivable that the concentration of serum Vpr (before clearance by cellular uptake and humoral immune response) should be in a range

close to that of the p24 antigen (23). Higher local concentrations Vpr would be predicted to exist in the intercellular space within lymph nodes, the most abundant site of viral replication. It is impossible at this time to predict the concentration of Vpr in serum or within lymphoid tissues, but studies are underway to measure extracellular Vpr in the lymph nodes and spleens of infected patients to understand better the role of soluble Vpr.

It has been suggested that free Vpr circulating in the peripheral blood is biologically active and may induce virion production from latently infected cells (24). Based on these data, several studies have focused on the biological activity of recombinant Vpr. The Vpr expressed in *E. coli* has been shown to induce apoptosis, an activity recently ascribed to Vpr in HIV-1-infected cells (15, 21, 51). However, in these studies, Vpr was excluded from the nucleus and embedded in the plasmalemma, possibly leading to the formation of ion conductive membrane pores (51). The *s*Vpr produced synthetically and analyzed in this study did not appear to be membrane-integrated but rather transduced cell membranes, was nucleophilic, and induced G_2 cell cycle arrest. The fact that the structure and purity of the recombinant protein studied previously (15, 21, 51) is unknown and that this product possessed no other known biological activity of viral Vpr implies that it was defective in its ability to fully traverse membranes and thus results in cytotoxic effects. Nevertheless, it will be interesting to examine whether *s*Vpr is able to mediate apoptosis (21, 22), an effect that may lead to T cell depletion and immune cell avoidance *in vivo*.

To this end, we hypothesize that *in vivo* soluble Vpr might arrest target cells in the G_2 phase of the cell cycle, a state known to be favorable for HIV production (12). However, from our results it is evident that Vpr is also able to transduce cells that are not targets of HIV infection. Therefore, the role of serum Vpr may be broader than promoting virus replication in latently infected cells (24). We hypothesize that the uptake of free Vpr would most likely occur in lymph nodes, where HIV replication is most concentrated. Therefore, extracellular Vpr might induce G_2 arrest, a cellular state known to promote apoptosis (21, 22), in cytotoxic T_{CD8} cells specific for HIV determinants. This would provide a mechanism of host immune cell evasion by HIV. These possibilities are currently under investigation.

Transduction of cells by *s*Vpr provides a novel mode of delivering proteins into the cytosol and the nucleus. This adds a new dimension to the possible role of cell transduction of designer proteins as therapeutic agents. Furthermore, this delivery system is quite efficient at nanomolar concentrations of *s*Vpr and does not require a protein denaturation step, a procedure required for high efficiency transduction by Tat (50). Of note, *s*Vpr retains its karyophilic properties and is able to induce G_2 cell cycle arrest in transduced cells. These findings add support to the notion that *in vivo* extracellular Vpr is biologically active.

*s*Vpr is highly immunogenic. We have used *s*Vpr to generate high titer and broadly reactive polyclonal and monoclonal antibodies reacting with Vpr. Furthermore, *s*Vpr activates HIV-1 replication in primary cells and is effectively incorporated into viral particles.[2] This, together with our finding that *s*Vpr is taken up from the extracellular medium, localizes to the nucleus, and induces G_2 cell cycle arrest, makes us confident that the peptide we have prepared displays biological activity. The availability of significant amounts of biologically active *s*Vpr should enable further studies aimed at clarifying the precise function of this viral protein, its mechanism of action, and its contributions to HIV pathogenesis.

[2] M. P. Sherman and U. Schubert, unpublished results.

Acknowledgments—We thank S. Weißflog for DLS, M. Nimtz for MS, Prisca Kunert for peptide synthesis, and David Sanan for confocal microscopy. We are indebted to J. W. Yewdell and J. R. Bennink for their continuous support.

REFERENCES

1. Lang, S. M., Weeger, M., Stahl-Hennig, C., Coulibaly, C., Hunsmann, G., Müller, J., Müller-Hermelink, H., Fuchs, D., Wachter, H., Daniel, M. M., Desrosiers, R. C., and Fleckenstein, B. (1993) *J. Virol.* **67,** 902–912
2. Gibbs, J. S., Lackner, A. A., Lang, S. M., Simon, M. A., Sehgal, P. K., Daniel, M. D., and Desrosiers, R. C. (1995) *J. Virol.* **69,** 2378–2383
3. Heinzinger, N. K., Bukrinsky, M. I., Haggerty, S. A., Ragland, A. M., Kewalramani, V., Lee, M.-A., Gendelman, H. E., Ratner, L., Stevenson, M., and Emerman, M. (1994) *Proc. Natl. Acad. Sci. U. S. A.* **91,** 7311–7315
4. Jenkins, Y., McEntee, M., Weis, K., and Greene, W. C. (1998) *J. Cell Biol.* **143,** 875–885
5. Vodicka, M. A., Koepp, D. M., Silver, P. A., and Emerman, M. (1998) *Genes Dev.* **12,** 175–185
6. Popov, S., Rexach, M., Zybarth, G., Reiling, N., Lee, M. A., Ratner, L., Lane, C. M., Moore, M. S., Blobel, G., and Bukrinsky, M. (1998) *EMBO J.* **17,** 909–917
7. Popov, S., Rexach, M., Ratner, L., Blobel, G., and Bukrinsky, M. (1998) *J. Biol. Chem.* **273,** 13347–13352
8. Bukrinsky, M., and Adzhubei, A. (1999) *Rev. Med. Virol.* **9,** 39–49
9. Emerman, M. (1996) *Curr. Biol.* **6,** 1096–1103
10. Levy, D. N., Fernandes, L. S., Williams, W. V., and Weiner, D. B. (1993) *Cell* **72,** 541–550
11. Rogel, M. E., Wu, L. I., and Emerman, M. (1995) *J. Virol.* **69,** 882–888
12. Goh, W. C., Rogel, M. E., Kinsey, C. M., Michael, S. F., Fultz, P. N., Nowak, M. A., Hahn, B. H., and Emerman, M. (1998) *Nat. Med.* **4,** 65–71
13. Poon, B., Grovit-Ferbas, K., Stewart, S. A., and Chen, I. S. Y. (1998) *Science* **281,** 266–269
14. Hrimech, M., Yao, X. J., Bachand, F., Rougeau, N., Cohen, E. A. (1999) *J. Virol.* **73,** 4101–4109
15. Piller, S. C., Ewart, G. D., Premkumar, A., Cox, G. B., and Gage, P. W. (1996) *Proc. Natl. Acad. Sci. U. S. A.* **93,** 111–115
16. Cohen, E. A., Terwilliger, E. F., Jalinoos, Y., Proulx, J., Sodroski, J. G., and Haseltine, W. A. (1990) *J. Acquired Immune Defic. Syndr.* **3,** 11–18
17. Stark, L. A., and Hay, R. T. (1998) *J. Virol.* **72,** 3037–3044
18. Felzien, L. K., Woffendin, C., Hottiger, M. O., Subbramanian, R. A., Cohen, E. A., and Nabel, G. J. (1998) *Proc. Natl. Acad. Sci. U. S. A.* **95,** 5281–5286
19. Wang, L., Mukherjee, S., Jia, F., Narayan, O., and Zhao, L.-J. (1995) *J. Biol. Chem.* **270,** 25564–25569
20. Kino, T., Gragerov, A., Kopp, J. B., Stauber, R. H., Pavlakis, G. N., and Chrousos, G. P. (1999) *J. Exp. Med.* **1,** 51–61
21. Stewart, S. A., Poon, B., Jowett, J. B., and Chen, I. S. (1997) *J. Virol.* **71,** 5579–5592
22. Ayyavoo, V., Mahboubi, A., Mahalingam, S., Ramalingam, R., Kudchodkar, S., Williams, W. V., Green, D. R., and Weiner, D. B. (1997) *Nat. Med.* **3,** 1117–1123
23. Levy, D. N., Refaeli, Y., MacGregor, R. R., and Weiner, D. B. (1994) *Proc. Natl. Acad. Sci. U. S. A.* **91,** 10873–10877
24. Levy, D. N., Refaeli, Y., and Weiner, D. B. (1995) *J. Virol.* **69,** 1243–1252
25. Macreadie, I. G., Castelli, L. A., Hewish, D. R., Kirkpatrick, A., Ward, A. C., and Azad, A. A. (1995) *Proc. Natl. Acad. Sci. U. S. A.* **91,** 27770–27774
26. Macreadie, I. G., Arunagiri, C. K., Hewish, D. R., White, J. F., and Azad, A. A. (1996) *Mol. Microbiol.* **19,** 1185–1192
27. Carpino, L. A. (1993) *Am. Chem. Soc.* **115,** 4397–4398
28. Wray, V., Federau, T., Henklein, P., Klabunde, S., Kunert, O., Schomburg, D., and Schubert, U. (1995) *Int. J. Pept. Protein Res.* **45,** 35–43
29. Adachi, A., Gentleman, H. E., König, S., Folks, T., Willey, R., Rabson, A., and Martin, M. A. (1986) *J. Virol.* **59,** 284–291
30. Moestrup, S. K., Birn, H., Fischer, P. B., Petersen, C. M., Verroust, P. J., Sim, R. B., Christensen, E. I., and Nexo, E. (1996) *Proc. Natl. Acad. Sci. U. S. A.* **93,** 8612–8617
31. Cornille, F., Wecker, K., Loffet, A., Genet, R., and Roques, B. (1999) *J. Peptide Res.* **54,** 427–435
32. Zhao, L. J., Wang, L., Mukherjee, S., and Narayan, O. (1994) *J. Biol. Chem.* **269,** 32131–32137
33. Selig, L., Pages, J. C., Tanchou, V., Preveral, S., Berlioz-Torrent, C., Liu, L. X., Erdtmann, L., Darlix, J., Benarous, R., and Benichou, S. (1999) *J. Virol.* **73,** 592–600
34. Bachand, F., Yao, X. J., Hrimech, M., Rougeau, N., and Cohen, E. A. (1999) *J. Biol. Chem.* **274,** 9083–9091
35. Kondo, E., Mammano, F., Cohen, E. A., and Göttlinger, H. G. (1995) *J. Virol.* **9,** 2759–2764
36. Schüler, W., Wecker, K., de Rocquigny, H., Baudat, Y., Sire, J., and Roques, B. P. (1999) *J. Mol. Biol.* **285,** 2105–2117
37. Luo, Z., Butcher, D. J., Murali, R., Srinivasan, A., and Huang, Z. (1998) *Biochem. Cell Biol.* **244,** 732–736
38. Yao, S., Azad, A. A., Macreadie, I. G., and Norton, R. S. (1998) *Protein Peptide Lett.* **5,** 127–134
39. Wecker, K., and Roques, B. P. (1999) *Eur. J. Biochem.* **266,** 359–369
40. Frankel, A. D., and Pabo, C. O. (1988) *Cell* **55,** 1189–1193
41. Lundgren, S., Carling, T., Hjalm, G., Juhlin, C., Rastad, J., Pihlgren, U., Rask, L., Akerstrom, G., and Hellman, P. (1997) *J. Histochem. Cytochem.* **45,** 383–392
42. Gras-Masse, H., Ameisen, J. C., Boutillon, C., Gesquiere, J. C., Vian, S., Neyrinck, J. L., Drobecq, H., Capron, A., and Tartar, A. (1990) *Int. J. Pept.*

Protein Res. **36,** 219–226
43. De Rocquigny, H., Petitjean, P., Tanchou, V., Decimo, D., Drouot, L., Delaunay, T., Darlix, J.-L., and Roques, B. P. (1997) *J. Biol. Chem.* **272,** 30753–30759
44. Roques, B. P., Morellet, N., de Rocquigny, H., Demene, H., Schüler, W., and Jullian, N. (1997) *Biochimie* (*Paris*) **79,** 673–680
45. Wang, L., Mukherjee, S., Narayan, O., and Zhao, L.-J. (1996) *Gene* (*Amst.*) **178,** 7–13
46. Nie, Z., Bergeron, D., Subbramanian, R. A., Yao, X. J., Checroune, F., Rougeau, N., and Cohen, E. A. (1998) *J. Virol.* **72,** 4104–4115
47. Zhang, S., Pointer, D., Singer, G., Feng, Y., Park, K., and Zhao, L. J. (1998) *Gene* (*Amst.*) **212,** 157–166
48. Green, M., Loewenstein, P. M. (1988) *Cell* **55,** 1179–1188
49. Schwarze, S. R., Ho, A., Vocero-Akbani, A., and Dowdy, S. F. (1999) *Science* **285,** 1569–1572
50. Nagahara, H., Vocero-Akbani, A. M., Snyder, E. L., Ho, A., Latham, D. G., Lissy, N. A., Becker-Hapak, M., Ezhevsky, S. A., and Dowdy, S. F. (1998) *Nat. Med.* **12,** 1449–1452
51. Piller, S. C., Ewart, G. D., Jans, P., Gage, P. W., and Jans, D. A. (1998) *Proc. Natl. Acad. Sci. U. S. A.* **95,** 4595–4600